RELATIONSHIP BETWEEN CONTROL-RELEVANT NONLINEARITY AND PERFORMANCE OBJECTIVE

Nicholas Hernjak * **Francis J. Doyle III** **,[1]
Frank Allgöwer *** **Tobias Schweickhardt** ***

* *Department of Chemical Engineering, University of Delaware, Newark, DE, USA*
** *Department of Chemical Engineering, University of California, Santa Barbara, CA, USA*
*** *Institut für Systemtheorie Technischer Prozesse, Universität Stuttgart, Stuttgart, Germany*

Abstract: In this work, the relationship between performance objective and control-relevant nonlinearity was investigated for Hammerstein and Wiener systems with polynomial nonlinearities. Nonlinearity assessment of the systems' inverses augmented with first-order linear filters using a numerical measure of nonlinearity showed that the nonlinearity varies depending on the relative magnitude of the filter time constant, but generally showed increasing nonlinearity with decrease in time constant. Similar assessment of the respective nonlinear internal model control structures indicated that the Hammerstein nonlinearity is weakly dependent on the filter time constant while the Wiener nonlinearity is strongly dependent.

Keywords: Nonlinear control systems, Nonlinear models, Performance analysis, Optimal control, Inverse system

1. INTRODUCTION

A key step in designing a control strategy for a process is determining the degree of complexity of the control algorithm necessary to optimally compensate for the intrinsic process nonlinearity (Ogunnaike *et al.*, 1993). As demonstrated previously (Hernjak *et al.*, 2002), certain nonlinear behaviors are more severe than others and some that appear significant in the open-loop setting may have little impact on closed-loop behavior.

Work involving use of the optimal control structure (OCS) as a means for assessing control-relevant nonlinearity (Stack and Doyle III, 1997) emphasized another issue of importance in deter-

mining the optimal degree of controller nonlinearity: the cost of the control action, or similarly, the desired level of performance of the controller. The implication of these results is that it is not only the inherent nonlinearity of the process that is of importance, but also the desired level of performance of the controller. In this work, a numerical measure of nonlinearity is employed to characterize the relationship between degree of controller nonlinearity and its performance objective for Hammerstein and Wiener systems with polynomial nonlinearities and scalar dynamics.

The particular control structures characterized in this work are nonlinear internal model control (IMC) algorithms. IMC algorithms involve the use of an explicit model of the process in order to compensate for uncertainty, including unmeasured disturbances (Morari and Zafiriou, 1989). Control

---

actions are generated from the disturbance prediction using an inverse of the model augmented with a unity-gain filter to maintain realizability. The filter time constant is introduced as a tuning parameter to adjust controller aggressiveness. Analysis of this type was suggested previously (Stack and Doyle III, 1999) using coherence as the measure of nonlinearity. Use of strictly linear IMC algorithms in determining the applicability of linear feedback for a process has also been investigated (Eker and Nikolaou, 2002). Other methods for analyzing control-relevant nonlinearity have also been proposed (Guay *et al.*, 1995).

In Section 2, the nonlinearity measure is introduced. In Section 3, the open-loop nonlinearity of the Hammerstein and Wiener structures is discussed. In Section 4, the nonlinearity of the model inverse plus filter is investigated. Finally, in Section 5, the nonlinearity of the classical IMC structure is analyzed.

2. NONLINEARITY MEASURE

The numerical nonlinearity measure proposed originally in (Allgöwer, 1995) and elaborated upon in (Helbig *et al.*, 2000) was used for nonlinearity characterization:

$$\phi_N^{\mathcal{U}} = \inf_{G \in \mathcal{G}} \sup_{\mathbf{u} \in \mathcal{U}} \frac{\| G[\mathbf{u}] - N[\mathbf{u}] \|_{P\mathcal{Y}}}{\| N[\mathbf{u}] \|_{P\mathcal{Y}}} \qquad (1)$$

where $N : \mathcal{U} \rightarrow \mathcal{Y}$ is the system operator and $G : \mathcal{U} \rightarrow \mathcal{Y}$ is a linear approximation to N. $\mathcal{U}$ is the space of considered input signals, $\mathcal{Y}$ is the space of admissible output signals, and $\mathcal{G}$ is the space of linear operators. $\phi_N^{\mathcal{U}}$ is a number between zero and one where a value of zero indicates the existence of a linear approximation to the system whose output matches the output of the original system over the set of inputs being considered. A value close to one indicates a highly nonlinear system.

As (1) represents an infinite dimensional optimization problem, approximate computational techniques are utilized to compute lower bounds on the measure. A general computational technique involves selecting a representative set of inputs and then building a linear approximation composed of a weighted sum of linear basis functions, e.g.:

$$y(s) = w_o u(s) + \sum_{i=1}^{N_l} \frac{w_i}{\tau_i s + 1} u(s) \qquad (2)$$

w_i are the weights on the basis functions, τ_i are the functions' time constants, and N_l is the number of basis functions chosen. It has been shown (Allgöwer, 1995) that the search for the

optimal set of w_i is convex. In this work, a quasi-Newton optimization algorithm with numerical Hessian update was employed to calculate the w_i.

A less rigorous but more computationally efficient lower bound on (1) can be obtained by limiting the space of admissible inputs to sinusoids of varying amplitude and frequency. Provided that the nonlinear system preserves periodicity, the output after any transients have decayed can be represented by a Fourier series:

$$y_s = A_o + \sum_{k=1}^{\infty} A_k \cdot \sin(k\omega t + \phi_k) \qquad (3)$$

By choosing the norm:

$$\|y(t)\| = \lim_{T \to \infty} \sqrt{\frac{1}{T} \int_0^T y^2(t) dt} \qquad (4)$$

it can be shown (Allgöwer, 1995) that the following is a lower bound on (1):

$$\chi_N^{\mathcal{U}_s} = \sup_{a \in \mathcal{A}, \omega \in \Omega} \sqrt{1 - \frac{A_1^2}{2A_o^2 + \sum_{k=1}^{\infty} A_k^2}} \qquad (5)$$

where $\mathcal{A}, \Omega$ are the sets of input signal amplitudes and frequencies being considered. $\chi_N^{\mathcal{U}_s}$ usually lies within 10-15% of the best value obtained through use of the optimization method discussed above.

3. OPEN-LOOP NONLINEARITY

The Hammerstein and Wiener models studied in this work consist of a first-order linear dynamic element with unity gain and time constant and a static polynomial nonlinearity of order n. The Hammerstein model is of the form:

$$v = u^n, \ \dot{x} = -x + v, \ y = x \qquad (6)$$

and the Wiener model is of the form:

$$v = u, \ \dot{x} = -x + v, \ y = x^n \qquad (7)$$

Hammerstein and Wiener model structures have been applied in modeling many nonlinear process systems (e.g., (Eskinat *et al.*, 1991), (Pottman and Pearson, 1996)) including pH systems and systems with nonlinear control valves.

The degree of open-loop nonlinearity for these systems is assessed using the LB (5). An input range of $0 \leq u(t) \leq 1$ centered at a steady-state of $u = 0.5$ is considered along with integer values of n ranging from 2 to 5. It is informative to consider the value of (5) computed at each frequency individually to study how different frequencies contribute to the nonlinearity measure,

as is plotted in Figures 1 and 2. This will be referred to as the frequency dependence of (5), but note that the true value of (5) is the maximum value of each of the curves. The results show that the frequency dependence of (5) follows opposite trends for the two systems with the Wiener system reaching its highest values at low frequency and the Hammerstein system approaching its highest values at high frequency. The results also indicate a trend of increasing nonlinearity with n.
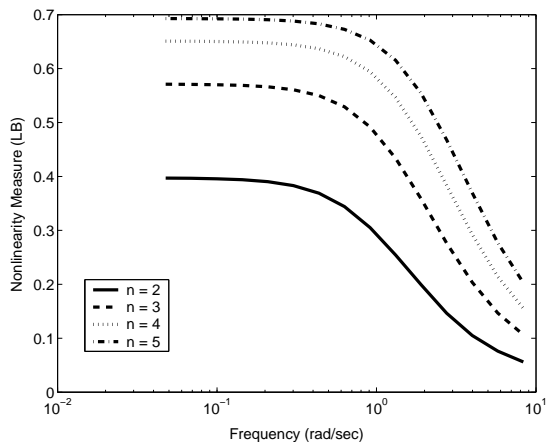
Fig. 1. Frequency dependence of Wiener system open-loop nonlinearity as measured using the LB (5) for various polynomial orders and an operating range of $0 \leq u(t) \leq 1$.
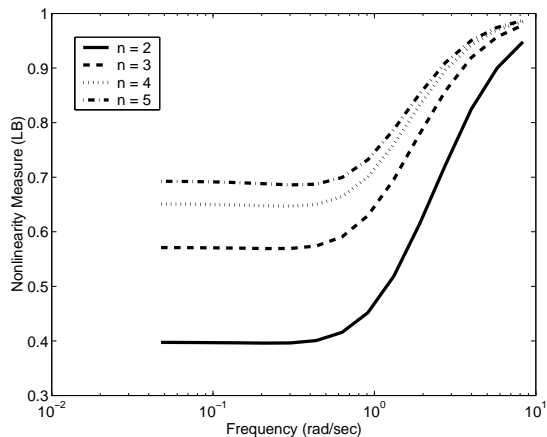
Fig. 2. Frequency dependence of Hammerstein system open-loop nonlinearity as measured using the LB (5) for various polynomial orders and an operating range of $0 \leq u(t) \leq 1$.

An analysis of the results in Figures 1 and 2 reveals that the low frequency results are identical for both systems. Because the low frequencies correspond to the region below the reciprocal time constant (1 rad/sec), these results correspond to the steady-state nonlinearity of the system, thus negating any effects of the linear dynamics and its placement in the structure.

The high frequency behavior is explainable by considering the frequency behavior of the linear dynamics. The linear dynamics are first order and therefore attenuate to an increasing degree the higher frequency inputs. As can be seen in Figure 3, for the Wiener system at high frequencies, the linear dynamics attenuate the single-frequency input to the point where the nonlinearity has little effect.

For the Hammerstein system, the static nonlinearity will first generate additional frequencies due to the ability of many nonlinear functions to generate harmonics (Pearson, 1999). The result of this, as can be seen in Figure 3, is that the final output exhibits a large positive bias from the steady-state value due to the linear dynamics not attenuating the zero-frequency harmonic (steady-state bias) generated by the static nonlinearity. This bias adds greatly to the value of the nonlinearity measure.
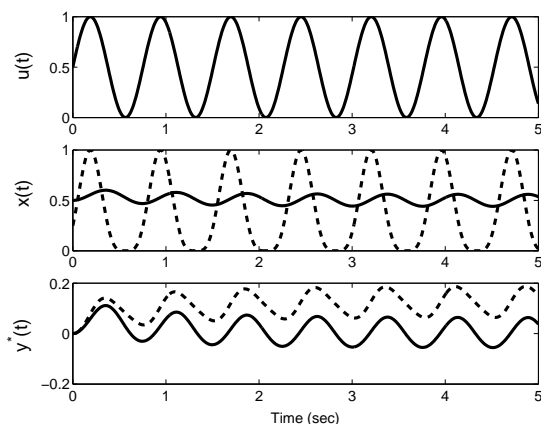
Fig. 3. Wiener (solid) and Hammerstein (dashed) systems time-domain signals for an input sinusoid of amplitude 0.5 and frequency 8.33 rad/sec when $n = 2$. $y^*(t)$ is the deviation from the steady-state output.

The results provided in this section are generalizable to other static nonlinearities and linear dynamics with only slight modifications as they rely only on the generation of harmonics by a nonlinear system and the attenuation characteristics of the dynamics.

4. SYSTEM INVERSE NONLINEARITY

In the linear IMC framework, its ISE optimal control results from the use of specific filters (which depend on input characteristics) coupled with the appropriate model inverse. While the optimality properties do not transfer directly to nonlinear IMC structures, these structures are still important for control-relevant analysis since they maintain many of the useful qualities of linear IMC structures (Economou *et al.*, 1986). The equivalent classical controller designs arising from IMC algorithms for the Hammerstein and

Wiener systems are shown in Figures 4 and 5. As outlined in the figures, the nonlinearity of the individual elements of these control structures and the overall structures themselves are considered separately in the sections of this paper. In this section, the nonlinearity of just the process inverse is considered as this structure corresponds to the IMC algorithm in the ideal case when there is no model error or output disturbances. In that case, the process inverse serves as an open-loop controller relating setpoint changes to manipulated variable moves.
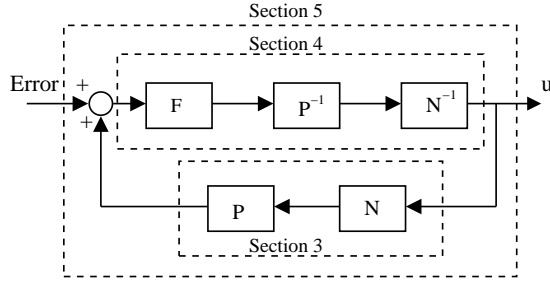
Fig. 4. Classical control structure corresponding to IMC design for a Hammerstein system. P = linear dynamics, N = static nonlinearity, F = filter.
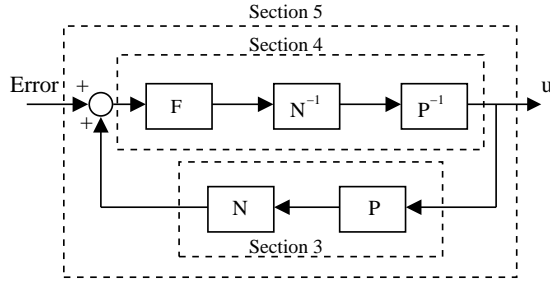
Fig. 5. Classical control structure corresponding to IMC design for a Wiener system. P = linear dynamics, N = static nonlinearity, F = filter.

To ensure realizability, the inverse is augmented with a first-order filter:

$$F(s) = \frac{1}{\lambda s + 1} \qquad (8)$$

where λ is the filter time constant. A first-order design is the minimum filter order necessary in this case to maintain realizability. Higher order filters could be designed but would correspond to controller designs with sluggish dynamic properties.

As seen in Figure 4 (Hammerstein structure), the inverse of the linear dynamics for a first-order system augmented with the filter is a lead-lag system, i.e.:

$$FP^{-1}(s) = \frac{s + 1}{\lambda s + 1} \qquad (9)$$

Therefore, the frequency behavior of the system is a function of the filter time constant. For large λ, the lag behavior of the system dominates and the high-frequency signals are attenuated, while for small λ, the lead behavior dominates and the high-frequency signals are magnified. Similar observations can be made for the Wiener system, but note that the filter and the inverse linear dynamics are separated by the inverse of the static nonlinearity. The nonlinearity of the inverse systems is considered in the range $0 \leq y(t) \leq 1$ centered at $y = 0.5$.

The effects of the lead-lag element on the nonlinearity can be seen for the Hammerstein system in Figure 6. At large λ values, the lag behavior dominates and the nonlinearity follows the Wiener trend seen in Figure 2. At small λ, the lead behavior dominates and there exists a maximum nonlinearity in the middle of the frequency range. It should be noted that, at low frequency, all of the curves in Figure 6 asymptote to the nonlinearity of the static nonlinearity block. Figure 7 is the corresponding plot for the Wiener inverse, demonstrating the same trend as the open-loop Wiener system for large λ and a completely different trend for low λ. The large λ trend is expected as the filter placement causes the first two blocks of the inverse to resemble a Wiener system of their own with a time constant that will dominate that of the inverse linear dynamics. Note that, for the Wiener system, the $\lambda = 1$ trend is not flat thus showing the effect of placing the nonlinearity between the two linear dynamic blocks.
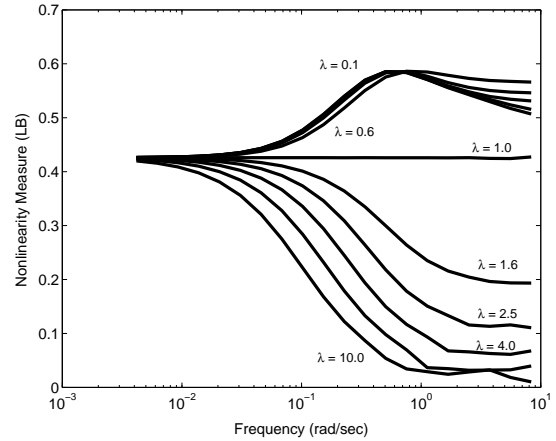
Fig. 6. Inverse Hammerstein system ($n = 3$) nonlinearity as a function of frequency for various values of the filter time constant, λ.

By the definition of (5), the true nonlinearity of the inverse system is the maximum value over the frequency range for each value of λ. Figure 8 shows these results for both systems. For the Hammerstein system, the inverse's nonlinearity is a weak function of λ over selected intervals. For $\lambda \geq 1$, the nonlinearity is that of the static nonlinearity block and for $\lambda < 1$, the nonlinearity
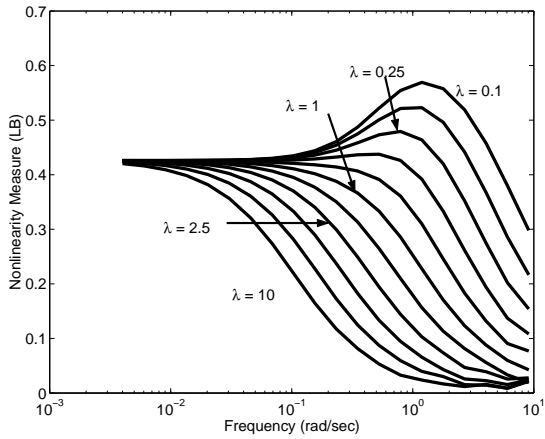
Fig. 7. Inverse Wiener system ($n = 3$) nonlinearity as a function of frequency for various values of the filter time constant, λ.

is that of the peak value shown in Figure 6. For the Wiener inverse, the nonlinearity matches that of the Hammerstein system for $\lambda > 1$ and steadily grows for $\lambda < 1$.
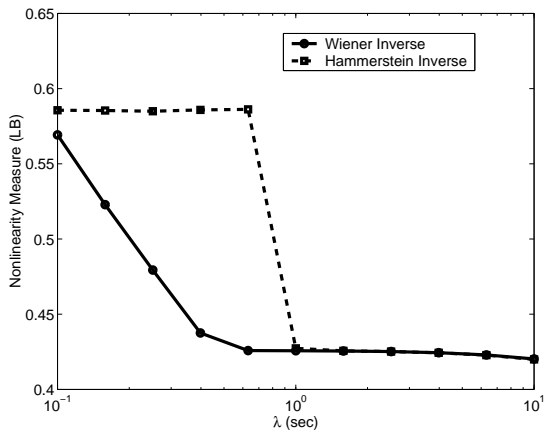
Fig. 8. Wiener and Hammerstein systems ($n = 3$) inverse nonlinearity as a function of the filter time constant, λ.

The conclusion that can be drawn from the data presented in this section is that the nonlinearity of these system inverses is dictated by the time constant of the linear filter (i.e., the closed-loop time constant). As the filter time constant varies in magnitude relative to the system's open-loop time constant, the severity of the nonlinearity changes in differing manners. Admittedly, consideration of λ values greater than one is not of much practical relevance since such tunings would correspond to a closed-loop time constant that is larger than the open-loop time constant. It is informative to consider the $\lambda > 1$ case since the overall results indicate a trend of increasing nonlinearity as one proceeds from the $\lambda > 1$ region to the $\lambda < 1$ region, corresponding to an increase in desired controller performance.

5. CLASSICAL CONTROL STRUCTURE NONLINEARITY

The final step in the control analysis is to consider the classical realization of the IMC controller. As shown in Figures 4 and 5, the input considered now is the setpoint error ($y_d - y$, where y_d is the set-point). This form of the IMC design is referred to as the "classical" realization, equivalent to the form of PID and other standard control algorithms in which setpoint error is the input and manipulated variable value is the output.

As is desired for this realization, the controllers will integrate the input (error) signals. For instance, for the Hammerstein structure, the N^{-1} block can be moved beyond the loop leaving a purely linear loop. In that case, it can be shown that the equivalent loop operator has the form:

$$L(s) = \frac{s + 1}{\lambda s} \qquad (10)$$

containing integral action. For the Wiener case, the P^{-1} block can be moved beyond the loop first followed by the N^{-1} block leaving only the filter in the feedback loop. The loop operator thus reduces to $1/\lambda s$, again showing integral action. The preceding analysis also demonstrates that the classical structures have the same general structures as the process inverses, i.e., the Hammerstein controller has a Wiener structure and the Wiener controller has a "linear-nonlinear-linear" block sandwich structure.

Given the integrating nature of the systems, the LB formulation of the nonlinearity measure cannot be used. Instead, the optimization-based algorithm discussed in Section 2 was used to characterize the system nonlinearity for a finite time horizon. Twenty stochastic input signals were implemented spanning the same magnitude and frequency ranges of $u(t)$ used to characterize the inverse system nonlinearity. The basis functions chosen for the linear approximation included one pure integrator and two unstable functions (i.e., $\tau_i < 0$) to account for any other positive feedback-induced behaviors of the system as well as 13 stable first-order lags with logarithmically-spaced $\tau_i \in [0.075, 60]$.

Figure 9 includes the results of the classical IMC nonlinearity assessment. The slight roughness of the trends in Figure 9 is due to the stochastic nature of the input signals. Signals with more precisely designed frequency content would result in smoother trends.

The Hammerstein system nonlinearity in Figure 9 is essentially invariant with respect to λ, which is consistent with the results for the inverse nonlinearity in Figure 8. The result in this case is due to the role of λ in the loop operator (10) in which
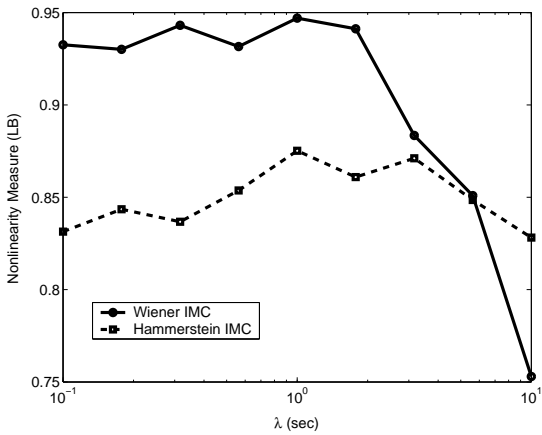
Fig. 9. Nonlinearity of the classical IMC structures as functions of the filter tuning parameter, λ.

it acts purely as a gain, therefore affecting all frequency components uniformly. For the Wiener system, the results in Figure 9 suggest a uniformly high nonlinearity for the $\lambda < 1$ region and a sharp decrease beyond $\lambda = 1$ again indicating decreased nonlinearity with detuning. In general, the results indicate that the nonlinearity of the controller necessary to effectively control either of these systems is quite high.

6. CONCLUSIONS

The results of this work demonstrate that the performance objective of a controller can greatly impact the control-relevant nonlinearity of the system. It was shown that the degree of nonlinearity of the process inverses and the classic realizations of the IMC controller is strongly dependent on the relative magnitude of the filter time constant as compared to the open-loop time constant for Wiener systems and, at most, weakly dependent for Hammerstein systems.

The results in Section 3 showed that the open-loop nonlinearity of the Hammerstein systems is generally greater than that of the Wiener systems. In comparing these results to the control-relevant results, it is suggested that the high Hammerstein open-loop nonlinearity mandates a uniformly high controller nonlinearity to optimally control these systems. For the Wiener systems, highly nonlinear control is only necessary when high levels of performance are desired. Therefore, at least in regards to IMC design, these common classes of systems are representative of two different cases:

(1) highly nonlinear open-loop systems that require highly nonlinear control for optimal performance (Hammerstein),
(2) mildly nonlinear open-loop systems that require highly nonlinear control *only* when high levels of performance are required (Wiener).

7. ACKNOWLEDGMENTS

8. REFERENCES

Allgöwer, F. (1995). Definition and computation of a nonlinearity measure. In: *3rd IFAC Nonlinear Control Systems Design Symposium*. Lake Tahoe, CA. pp. 279–284.

Economou, C. G., M. Morari and B. O. Palsson (1986). Internal model control. 5. Extension to nonlinear systems. *Ind. Eng. Chem., Process Des. Dev.* **25**, 403–411.

Eker, S. A. and M. Nikolaou (2002). Linear control of nonlinear systems - the interplay between nonlinearity and feedback. *AIChE J.* **48**(9), 1957–1980.

Eskinat, E., S. H. Johnson and W. L. Luyben (1991). Use of Hammerstein models in identification of nonlinear systems. *AIChE J.* **37**(2), 255–268.

Guay, M., P.J. McLellan and D.W. Bacon (1995). Measurement of nonlinearity in chemcial process control systems: The steady state map. *Can. J. Chem. Eng.* **73**, 868–882.

Helbig, A., W. Marquardt and F. Allgöwer (2000). Nonlinearity measures: Definition, computation and applications. *J. Process Contr.* **10**, 113–123.

Hernjak, N., F. J. Doyle III and R. K. Pearson (2002). Control-relevant characterization of nonlinear classes of process systems. In: *Proc. IFAC World Congress*. Barcelona.

Morari, M. and E. Zafiriou (1989). *Robust Process Control*. Prentice-Hall, Englewood Cliffs, NJ.

Ogunnaike, B. A., R. K. Pearson and F. J. Doyle III (1993). Chemical process characterization: With applications in the rational selection of control strategies. In: *Proceedings of the European Control Conference*. Groningen, The Netherlands. pp. 1067–1071.

Pearson, R. K. (1999). *Discrete-Time Dynamic Models*. Oxford University Press. New York.

Pottman, M. and R.K. Pearson (1996). Gray-box modelling of processes with output multiplicities. In: *IFAC World Congress*. San Francisco, USA. pp. 67–72.

Stack, A. J. and F J. Doyle III (1997). Application of a control-law nonlinearity measure to a chemical reactor. *AIChE J.* **43**, 425–447.

Stack, A. J. and F. J. Doyle III (1999). Local nonlinear performance assessment for single controller design. In: *Proc. IFAC World Congress*. Beijing. pp. 111–117.